The Lorenz function: Its properties at optimum thermoelectric figure-of-merit

E. Flage-Larsen[a] and Ø. Prytz
Department of Physics, University of Oslo, P. O. Box 1048, NO-0316 Oslo, Norway

(Received 14 May 2011; accepted 5 October 2011; published online 16 November 2011)

The Lorenz function is investigated for different scattering mechanisms, temperatures, chemical potentials, and charge carrier concentrations. We show that at optimum thermoelectric figure-of-merit, the deviation from the degenerate and non-degenerate limits is significant, where the magnitude of the deviation is determined by the scattering mechanism. Furthermore, the Lorenz functions are parameterized as a function of charge carrier concentration, temperature, and effective mass for different scattering mechanisms. © *2011 American Institute of Physics*. [doi:10.1063/1.3656017]

The past decade has seen a resurgence of research into thermoelectric materials and their applications. The increased interest is largely driven by the opportunity to generate electricity from waste heat. The efficiency of the thermoelectric conversion process is governed by the dimensionless figure-of-merit $zT = \alpha^2\sigma T/\kappa$, where α, σ, κ, and T are the Seebeck coefficient, electrical conductivity, thermal conductivity, and temperature, respectively. The thermal conductivity has two contributions: heat conduction in the lattice (κ^l) and heat conduction by the charge carriers (κ^e), hereafter termed the electronic thermal conductivity.

Early discussions of the Lorenz number, which relates the electronic thermal and electrical conductivity, can be found in the textbook by Wilson[1] and references therein. A more in-depth theoretical work on the Lorenz number was later performed by Price.[2] There have since been numerous studies that confirm deviations[3–9] from the Sommerfeld limit[1] defined for simple degenerate metals obeying elastic scattering.

The Lorenz function is particularly important for thermoelectrics, where it serves to separate the electronic thermal and lattice thermal conductivity. Modern thermoelectric materials often display a high degree of structural and electronic complexity, and there is in general no reason to expect the Sommerfeld value[1] to hold for these materials. Since the majority of the optimizations of thermoelectric materials involve modifications to the electrical conductivity or lattice thermal conductivity, precise knowledge of this function is important to make a sound analysis of the interdependence and trends across modifications.

In the present work, we analyze the Lorenz function for different scattering mechanisms and temperatures. Particular emphasis is placed on applications to thermoelectric materials, and a parametrization of the Lorenz function is developed to allow quantitative estimates of the Lorenz number without solving the transport equations.

The Boltzmann transport equations are extensively covered in textbooks, see, for example, Ashcroft and Mermin.[10] We will here only repeat the tensors involved in the calculation of the Lorenz function for the sake of completeness. The electronic thermal conductivity in its full form is defined as

$$\kappa^e_{ij} = \kappa^0_{ij} - T\chi_{ik}\alpha_{kj}. \tag{1}$$

The first term is defined as $\kappa^0_{ij} = \Sigma^2_{ij}/e^2T$, while $\chi_{ij} = \Sigma^1_{ij}e/T$. The electrical conductivity is similarly defined as $\sigma_{ij} = \Sigma^0_{ij}e^2$ and the Seebeck coefficient as $\alpha_{ij} = (\sigma)^{-1}_{ik}\chi_{kj}$, where $\Sigma^p_{ij} = \sum_n \Sigma^{p,n}_{ij}$ and

$$\sum_{ij}^{p,n} = \frac{1}{\Omega}\int (\epsilon^n(\vec{k}) - \mu)^p \tau^n(\vec{k}) v^n_i(\vec{k}) v^n_j(\vec{k}) \left(-\frac{\partial f}{\partial \epsilon^n(\vec{k})}\right) d\vec{k}. \tag{2}$$

Here, $\epsilon^n(\vec{k})$ is the energy of the nth charge carrier with wave vector $\vec{k}$, $\vec{v}$ its velocity, μ the chemical potential, f the equilibrium Fermi distribution function, and e the electronic charge. The reciprocal integration volume is defined by Ω. The ratio of the electronic thermal to electrical conductivity yields the Lorenz tensor L as

$$L_{ij} = \frac{1}{T}\kappa^e_{ik}(\sigma)_{kj}{}^{-1} \tag{3}$$

or $L = \frac{\kappa^0}{T\sigma} - \alpha^2$. For metals or degenerate systems, $\alpha \to 0$ and $\chi \to 0$, due to a small change in the density of states part of the transport distribution function as a function of energy. This function contains the density of states, band velocities, and scattering parameters. To leading order, κ^0 will thus determine the electronic thermal properties for metals. However, for semiconductors, systems with complex electronic structures or in general systems falling between the degenerate and non-degenerate limit,[11] corrections due to a non-vanishing changes in the transport distribution function as a function of energy will be of importance.[2,10] Deviations from the Sommerfeld value will also be caused by scattering effects. In particular, inelastic electron scattering causes significant corrections, even for metals.[2] All such corrections are highly relevant for thermoelectric materials.

Motivated by this, we calculate the corrections to the Lorenz number between the degenerate and non-degenerate limit for different elastic scattering mechanisms. Parabolic band behavior is assumed, with energy dispersion of $\epsilon = \hbar^2k^2/2m^*(m^* = am_e)$ and carrier velocity $\vec{v} = \hbar\vec{k}/m^*$. Elastic scattering effects are incorporated by assuming the relaxation time approximation[10] and an energy and temperature dependent relaxation time,[11] i.e., $\tau(\epsilon, T) = \tau_0(\epsilon/k_bT)^{r-1/2}$, where r is 0, 2, and 1/2 for acoustic phonon, ionized impurity, and constant scattering time mechanisms, respectively.[11] The

[a]Electronic mail: espen.flage-larsen@fys.uio.no.

scattering prefactor τ_0 is fixed at 1 fs and Matthiessen's rule is used to combine different scattering mechanisms. Note that the Seebeck coefficient and Lorenz function are independent of the effective mass as a function of chemical potential. However, the effective mass dependent relation between the chemical potential and carrier concentration is easily evaluated.[10] Unless otherwise stated, the temperature is 300 K.

The Lorenz number as a function of chemical potential (μ) and carrier concentration (n_c) is calculated for three different scattering mechanisms, see Fig. 1. In the degenerate limit, i.e., high carrier concentrations, the Lorenz function approaches the Sommerfeld limit, $L_0 = 2.443 \times 10^{-8}$ V^2/K^2. In the non-degenerate limit, three distinctly different asymptotes, hereafter L_∞, depending on the type of scattering mechanism are present. For a parabolic band, regardless of the scattering mechanism and effective mass,[11] the Lorenz values falls between 1.48 and 2.97 $\times 10^{-8}$ V^2/K^2. The deviations from the Sommerfeld value are most severe for acoustic phonon scattering.

The deviations from the Sommerfeld value have significant implications for thermoelectric materials whose performance is determined by the dimensionless figure-of-merit. The aim is to align the carrier concentration at the calculated (or extrapolated) figure-of-merit maximum, z_mT. This is thus a good reference point for an analysis of the Lorenz values, not the degenerate and/or non-degenerate limits. In Fig. 1, the maxima of the figure-of-merit for a constant lattice thermal conductivity, $\kappa^l = 1$ W/Km are indicated by the vertical lines. The Lorenz values at z_mT are summarized in Table I together with the relative deviation ΔL from the Sommerfeld value L_0. For ionized impurity scattering, the difference is small and the Sommerfeld value can be considered an acceptable approximation. However, for the three other scattering mechanisms, and, in particular, for acoustic phonon scattering, there are up to 45% deviations from the Sommerfeld value. Such deviations can significantly burden the analysis of trends in κ^e based on measurements of κ^l and care should be taken to use appropriate Lorenz values. If minority carrier conduction is present, bipolar conduction will also be of importance.

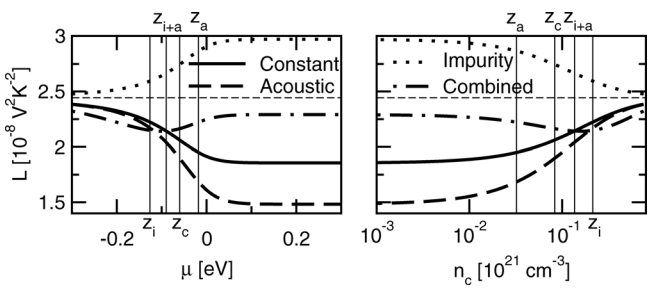

FIG. 1. Lorenz function at different chemical potentials and carrier concentrations for a single parabolic band. Three limiting electron scattering mechanisms are shown: constant relaxation time (solid line), acoustic phonon (dashed line), and ionized impurity (dotted line). The figure-of-merit maximum (for $\kappa^l = 1$ W/Km, $a = -1$) is indicated for the three scattering mechanisms: z_a, z_i, and z_c for acoustic phonon, ionized impurity, and constant relaxation time scattering, respectively. A mixture of acoustic phonon and ionized impurity scattering (dashed-dotted) is also included with the scattering prefactor defined as $\tau_0^a/\tau_0^i = 50$. The Sommerfeld limit is illustrated by the thin dashed line. The band onset is at 0 eV.

TABLE I. The Lorenz value L and deviation $\Delta L = |L - L_0|/L$ from the Sommerfeld value L_0 at the optimized figure-of-merit, z_mT for different scattering mechanisms. The combined scattering is calculated for $\tau_0^a/\tau_0^i = 50$. Fitting coefficients A_i for Eq. (4) are also listed.

	L	ΔL	L_∞	A_1
Constant	2.061	1.185	1.856	−0.007070
Acoustic	1.686	0.449	1.485	0.067228
Impurity	2.595	0.059	2.970	−0.948436
Combined	2.142	0.141	—	—
		A_2	A_3	A_4
Constant		-7.139721×10^3	−0.993498	6.706518×10^1
Acoustic		-5.346788×10^3	−1.065720	-3.922918×10^2
Impurity		1.395837×10^3	−0.062829	-1.449908×10^4

As the integrals in the Boltzmann transport tensors have no general analytic solutions, numerical analyses of the Lorenz function are needed for each particular material. However, we have developed a parameterization of the data in Fig. 1 which can be used to estimate the Lorenz number for a particular case. The Lorenz function can be described as

$$L(n_c) = L_0 + \frac{(L_\infty - L_0)(1 + A_1 + A_3)}{1 + A_1 e^{A_2 b n_c} + A_3 e^{A_4 b n_c}}, \qquad (4)$$

where L_∞ and L_0 are the non-degenerate and Sommerfeld Lorenz values, respectively, in units of 10^{-8} V^2/K^2. The coefficients A_i are parameters listed in Table I for each scattering mechanism. These parameters yield RMS errors below 0.1% compared to the numerical solution. The ratio $(aT)^{-3/2} = b$ determines the shift in the carrier concentration, n_c (in units of 10^{21} cm^{-3}, valid in the $(-\infty, \infty)$ range) for a change in effective mass and/or temperature, T (in K). This parametrization is valid for a general set of systems described by a single parabolic band and an appropriate scattering model. To illustrate this, we calculate the Lorenz number versus temperature for five different materials, see Fig. 2. An agreement between the calculated Lorenz values from the Fermi integrals (see Refs. 12 and 13) and the parameterization is expected and observed. For the skutterudites and the 14-1-11 Zintl's, it is common to use 2 and 2.443 $\times$ 10^{-8} V^2/K^2 for the Lorenz number (see Refs. 14, 15 and 16), respectively. The parametrization here shows that these values are most likely an overestimation.

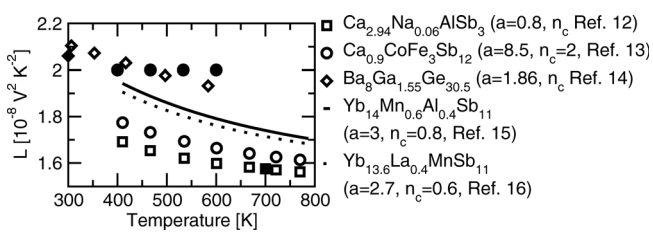

FIG. 2. Parametrized Lorenz values as a function of temperature. The filled square ($Ca_{2.94}Na_{0.06}AlSb_3$ (Ref. 12), circle ($Ce_{0.9}CoFe_3Sb_{12}$ (Ref. 14), and diamond ($Ba_8Ga_{15.5}Ge_{30.5}$ (Ref. 13) show the Lorenz values calculated from experimental data and used to extract the electronic thermal conductivity at the given temperature. A temperature independent effective mass ($a = m^*/m_e$) and acoustic phonon scattering are assumed. The carrier concentration n_c (in units of 10^{21} cm^{-3}) is listed, unless it has been extracted from temperature dependent data (see references).

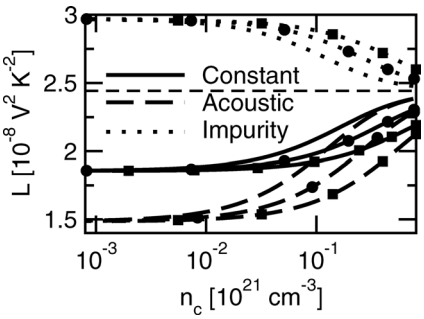

FIG. 3. Lorenz values as a function of carrier concentrations, temperatures (no symbol 300 K, circles 500 K, and squares 800 K) and different scattering mechanisms (see caption of Fig. 1 for additional details).

From Eq. (3), we see that the Lorenz function has an explicit T^{-1} dependence. In addition, the transport tensors are also temperature dependent and we should therefore expect additional variations of the Lorenz number with temperature. This is confirmed in Fig. 2. In Fig. 3, the Lorenz values are calculated as a function of carrier concentration, temperature, and different scattering mechanisms. Based on this, it is important to emphasize on the importance of calculating the Lorenz number at different temperatures, carrier concentrations, and effective masses and not use a single value throughout a study dependent on these parameters.

The location of z_mT will also change with temperature. We have calculated the Lorenz number for some representative temperatures at z_mT (see Table II). These reveal only small variations for T between 300 and 800 K. The temperature variation is largest and increasing for ionized impurity scattering, while the temperature dependency is weaker and close to non-existent for the acoustic phonon and constant scattering mechanisms. Even though the temperature dependence is relatively weak at z_mT and dominated by changes in the carrier concentration, systems with, e.g., temperature dependent band structures (i.e., change of band curvature) or complex scattering properties might additionally need careful evaluation of the Lorenz values at different temperatures.

TABLE II. Temperature dependence of the Lorenz values (L_c, L_a and L_i for constant, acoustic phonon and ionized impurity scattering, respectively) at z_mT.

Temperate [K]	L_c	L_a	L_i
300	2.061	1.686	2.595
500	2.044	1.686	2.701
800	2.012	1.666	2.799

We would like to acknowledge the Norwegian Research Council for financial support and Terje G. Finstad and Johan Taftø for discussions.

[1]A. H. Wilson, *The Theory of Metals* (Cambridge University Press, London, 1958).
[2]P. J. Price, IBM J. Res. Dev. **1**, 147 (1957).
[3]G. S. Kumar and G. Prasad, J. Mater. Sci. **28**, 4261 (1993).
[4]M. G. Vavilov and A. D. Stone, Phys. Rev. B **72**, 205107 (2005).
[5]L. V. Prokof'eva, A. A. Shabaldin, V. A. Korchagin, S. A. Nemov, and Y. I. Ravich, Semiconductors **42**, 1161 (2007).
[6]Z. Bian, M. Zebarjadi, R. Singh, Y. Ezzahri, A. Shakouri, G. Zeng, J.-H. Bahk, J. E. Bowers, J. M. O. Zide, and A. C. Gossard, Phys. Rev. B **76**, 205311 (2007).
[7]M. N. Ou, T. J. Yang, S. R. Harutyunyan, Y. Y. Chen, C. D. Chen, and S. J. Lai, Appl. Phys. Lett. **92**, 063101 (2008).
[8]A. Garg, D. Rasch, E. Shimshoni, and A. Rosch, Phys. Rev. Lett. **103**, 096402 (2009).
[9]R. Xia, J. L. Wang, R. Wang, X. Li, X. Zhang, X.-Q. Feng, and Y. Deng, Nanotechnology **21**, 085703 (2010).
[10]N. W. Ashcroft and N. D. Mermin, *Solid State Physics* (Brooks/Cole Thomson Learning, Pacific Grove, 1976).
[11]V. I. Fistul, *Heavily Doped Semiconductors* (Translated from Russian by Albin Tybulewicz) (Plenum, New York, 1969).
[12]A. Zevalkink, E. S. Toberer, W. G. Zeier, E. Flage-Larsen, and G. J. Snyder, Energy Environ. Sci. **4**, 510 (2010).
[13]A. F. May, E. S. Toberer, A. Saramat, and G. J. Snyder, Phys. Rev. B **80**, 125205 (2009).
[14]B. C. Sales, D. Mandrus, B. C. Chakoumakos, V. Keppens, and J. R. Thompson, Phys. Rev. B **56**, 15081 (1997).
[15]E. S. Toberer, C. A. Cox, S. R. Brown, T. Ikeda, A. F. May, S. M. Kauzlarich, and G. J. Snyder, Adv. Funct. Mater. **18**, 2795 (2008).
[16]E. S. Toberer, S. R. Brown, T. Ikeda, S. M. Kauzlarich, and G. J. Snyder, Appl. Phys. Lett. **93**, 062110 (2008).